



Quenching of chlorophyll fluorescence induced by silver nanoparticles



A.M. Queiroz^{a,b}, A.V. Mezacasa^b, D.E. Graciano^b, W.F. Falco^b, J.-C. M'Peko^c, F.E.G. Guimarães^c, T. Lawson^d, I. Colbeck^d, S.L. Oliveira^a, A.R.L. Caires^{a,*}

^a Grupo de Óptica e Fotônica, Instituto de Física, Universidade Federal de Mato Grosso do Sul, CP 549, 79070-900 Campo Grande, MS, Brazil

^b Grupo de Óptica Aplicada, Universidade Federal da Grande Dourados, CP 533, 79804-970 Dourados, MS, Brazil

^c Instituto de Física de São Carlos, Universidade de São Paulo, CP 369, 13560-970 São Carlos, SP, Brazil

^d School of Biological Sciences, University of Essex, Wivenhoe Park, CO4 3SQ Colchester, Essex, United Kingdom

ARTICLE INFO

Article history:

Received 21 January 2016

Received in revised form 19 May 2016

Accepted 22 May 2016

Available online 25 May 2016

Keywords:

Chlorophyll

Fluorescence

Lifetime

Quenching

Silver

Nanoparticle

ABSTRACT

The interaction between chlorophyll (Chl) and silver nanoparticles (AgNPs) was evaluated by analyzing the optical behavior of Chl molecules surrounded by different concentrations of AgNPs (10, 60, and 100 nm of diameter). UV–Vis absorption, steady state and time-resolved fluorescence measurements were performed for Chl in the presence and absence of these nanoparticles. AgNPs strongly suppressed the Chl fluorescence intensity at 678 nm. The Stern–Volmer constant (K_{SV}) showed that fluorescence suppression is driven by the dynamic quenching process. In particular, K_{SV} was nanoparticle size-dependent with an exponential decrease as a function of the nanoparticle diameter. Finally, changes in the Chl fluorescence lifetime in the presence of nanoparticles demonstrated that the fluorescence quenching may be induced by the excited electron transfer from the Chl molecules to the metal nanoparticles.

© 2016 Elsevier B.V. All rights reserved.

1. Introduction

The development of nanotechnologies in recent decades has led to an indiscriminate use of nanomaterials (NMs) in various industrial applications [1]. The concern about the impact of nanoparticles (NPs) in the environment has increased because their release and accumulation are inevitable [2]. NMs may constitute a toxicological risk as nanosized particles have presented toxicity in a variety of organisms, being generally more toxic than larger particles (bulk) [3]. In fact, NPs behave differently from bulk materials, with regard to chemical, physical and biological properties, due to a change in the nature of the interaction forces between NPs and environment. Consequently, the size of the NPs is a key feature in relation to the effects that NPs can induce in the environment, human health and biosphere as a whole [4].

Silver nanoparticles (AgNPs) are among the most used NPs for developing new technologies and commercial products due to their antimicrobial properties [7]. The wide variety of commercial applications of the AgNPs results in a significant increase in their production and, consequently, release to the environment [8,9]. Plants are particularly relevant in this scenario because of their constant interaction with the air, soil, and water so that they are potentially exposed to NPs. In addition, plants may represent a possible agent for NPs' bioaccumulation

and biomagnification due to their importance in the food chain since they are consumed by organisms of different trophic levels [5,6].

Recently, several studies about the impacts of AgNPs on plant development were reported. For instance, Ma et al. showed that AgNPs are toxic to seedlings of watercress even at low concentrations (<1 ppm) [6]. They observed that different concentrations of AgNPs with diameter between 20 and 80 nm affected plant growth and the nanoparticle phytotoxicity depends on the size and concentration of the AgNPs. In turn, Jiang et al. also demonstrated that AgNPs induced a significant decrease in the plant biomass, chlorophyll content and photosynthetic efficiency of photosystem II (Fv/Fm) in *Spirodela polyrrhiza* [10].

During photosynthesis, when light energy is converted into chemical energy by plants, the key role is played by chlorophyll *a* because it absorbs and transfers energy to the reaction centers, inducing charge separation and, subsequently, photosynthetic electron transport [11]. In addition, it is well established that chlorophyll fluorescence (ChlF) may be applied to evaluate the physiological status of plants, in vivo, [12–13] as chlorophyll molecule is an intrinsic fluorophore present in green plants. Consequently, ChlF can be used for monitoring, directly or indirectly, the environmental impact induced by biotic or abiotic agents as the photosynthetic efficiency of plants usually decreases when placed under a stress condition [14–17].

To obtain fundamental knowledge about interaction between Chl molecules and AgNPs and to evaluate the potential application of ChlF spectroscopy as an analytical technique for further investigation about nanoparticle effects on plants, the present study performed a close

* Correspondent author.

E-mail address: anderson.caires@ufms.br (A.R.L. Caires).

analysis of ChlF behavior, extracted from leaves of fava bean (*Vicia faba* L.), when surrounded by different diameters and concentrations of AgNPs.

2. Materials and methods

2.1. Silver nanoparticles

Silver nanoparticles (AgNPs) with spherical form at $0.02 \text{ mg} \cdot \text{mL}^{-1}$ ($185 \text{ } \mu\text{M}$) in aqueous buffer, containing sodium citrate as stabilizer, were purchased from Sigma-Aldrich (Brazil). As informed by the company, the nanoparticle diameters were determined by transmission electron microscopy (TEM) and the mean diameters of the used AgNPs were 100 ± 8 , 60 ± 8 , and $10 \pm 4 \text{ nm}$. Additional information of the AgNPs is presented in the Supplementary material (Fig. S1).

In all analyses performed, the AgNPs were suspended in a dilute aqueous citrate buffer for stabilizing the nanoparticles and to prevent aggregation. This buffer solution was selected because the citrate-based agent is weakly bound with the nanoparticle surface and can be readily replaced by other molecule, allowing a direct interaction between chlorophyll molecules and AgNPs surface.

2.2. Chlorophyll extract

Leaves of fava bean (*Vicia faba* L.) were collected and cut into small pieces. 30 mL of methanol PA was added for each 3 g of leaves and they were incubated for 72 h at 2°C . Then, chlorophyll extract was separated and stored in amber bottle at around 2°C . The chlorophyll content was determined by using the Arnon method adapted by Porra (Eq. 1) [18], where $A^{652.0}$ ($A^{665.2}$) is the absorbance value at 652.0 nm (665.2 nm) and 24.23 (3.26) obtained from the millimolar extinction coefficients of chlorophylls at 652.0 nm (665.2 nm) for simultaneous determination of the total chlorophyll content [$\text{Chl } a + b$], in μM units, in buffered methanol.

$$[\text{Chl } a + b] = 24.23A^{652.0} + 3.26A^{665.2} \quad (1)$$

2.3. Nanoparticle-chlorophyll solution

To study the interaction between chlorophyll and AgNPs, 0.5 mL of the chlorophyll extract at $14.7 \text{ } \mu\text{M}$ was added to 2.5 mL of the AgNPs-containing solution at concentrations of 2.4, 9.7, 38.6, 77.2, and $154.5 \text{ } \mu\text{M}$. The same procedure was carried out for the three nanoparticle sizes (10, 60, and 100 nm).

2.4. Optical analyses

The molecular absorption in the 200–800 nm wavelength range were performed in a Cary 50 UV-Vis spectrophotometer (Varian) using a quartz cuvette of 10 mm optical pathlength at room temperature.

The fluorescence measurements were performed using a fluorimeter consisting of a laser excitation source, a monochromator (2000 USB FL-OceanOptics), a Y-type optical fiber. The fluorescence spectra of the samples were obtained at wavelengths between 450 and 800 nm with excitation at 405 nm. All measurements were carried out at room temperature using a quartz cuvette with four polished faces and 10 mm optical pathlength.

Fluorescence lifetime measurements were performed using a multi-photon confocal microscope (Zeiss LSM 780) with a $20\times$ objective and single-photon avalanche diode detector with picosecond temporal resolution. A tunable 690–1100 nm laser (Chameleon, Coherent) was used as the excitation source. Lifetime measurements of the samples were taken at 678 nm with a two-photon excitation at 800 nm. The excitation laser provides 140-fs pulses with a repetition rate of 80 MHz.

3. Results and discussion

Fig. 1 shows the absorption and fluorescence spectra for the Chl extract in the absence of AgNPs. The Soret and $Q_{x,y}$ absorption bands were observed in the 400–450 and 600–750 nm wavelength ranges, respectively (Fig. 1a). In turn, a prominent emission band centered at 678 nm was observed along with a weak shoulder located around 728 nm (Fig. 1b) [19].

Absorption data of AgNPs not surrounded by Chl molecules were also collected. For instance, the absorption spectrum of the AgNPs of 60 nm is presented in Fig. 2a. An absorption band at around 430 nm due to the plasmon resonance induced by the collective oscillation of the electrons on the metal surface was observed [20]. Additionally, the UV-Vis absorption analysis revealed that the plasmon resonance is suppressed whether the pH of the solution is acid or basic, as presented in the Fig. S2 in the Supplementary materials. This result is possibly due to the formation of nanoparticle aggregation as pH is one of the most important factors in the formation of nanoparticle clusters [21].

Considering the previous finding, absorption spectra of the solutions with neutral pH containing AgNPs with different nanoparticle sizes and concentrations were acquired (data not show). Fig. 2b highlights the linear red-shift of the absorption peak of the AgNPs solution with increasing nanoparticle diameter (see the full spectra in Fig. S1 in the Supplementary materials). Similar results for metal nanoparticles were also verified elsewhere [22] as the absorption maximum of plasmon resonance shifts to higher wavelengths as nanoparticle size increase [22].

Fig. 2c displays that the plasmon absorption intensity linearly increased as a function of the AgNPs concentration, with R^2 coefficients of 0.9912, 0.9997, and 0.9972 for the diameter of 10, 60, and 100 nm, respectively. Besides, the angular coefficient obtained from Fig. 2c linearly decreases as a function of nanoparticle size presenting a R^2 coefficient of 0.9968 (Fig. 2d). In fact, these results may be accounted by the metal surface area dependence of the plasmon resonance [22]. For instance, it is known that the total metal surface area increases as nanoparticle concentration increases, enhancing of the plasmon resonance absorption (Fig. 2c) as well as the total metal surface area decreases as nanoparticle size increases, for a given nanoparticle concentration, reducing the plasmon resonance absorption (Fig. 2d) [22].

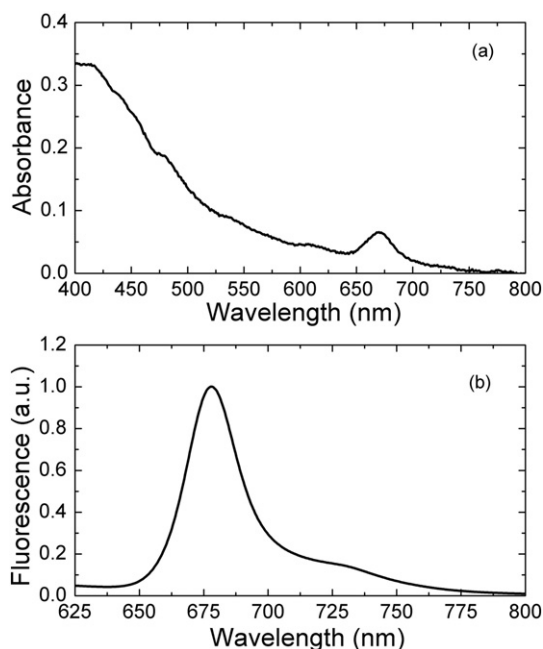


Fig. 1. (a) Absorption and (b) fluorescence spectrum of chlorophyll extract at $1.15 \text{ } \mu\text{M}$. The fluorescence spectrum was obtained by exciting at 405 nm.

Download English Version:

<https://daneshyari.com/en/article/1230410>

Download Persian Version:

<https://daneshyari.com/article/1230410>

[Daneshyari.com](https://daneshyari.com)